

John Carroll University

From the Selected Works of Peifang Tian

June 2, 1997

A surface-emitting vacuum-deposited organic light emitting device

V. Bulovic
Peifang Tian
P. E. Burrows
M. R. Gokhale
S. R. Forrest, et al.



Available at: https://works.bepress.com/peifang_tian/2/

A surface-emitting vacuum-deposited organic light emitting device

V. Bulović, P. Tian, P. E. Burrows, M. R. Gokhale, and S. R. Forrest
Department of Electrical Engineering, Center for Photonics and Optoelectronic Materials,
and Princeton Materials Institute, Princeton University, Princeton, New Jersey 08544

M. E. Thompson
Department of Chemistry, University of Southern California, Los Angeles, California 90089

(Received 20 February 1997; accepted for publication 1 April 1997)

We demonstrate a vacuum-deposited organic light emitting device which emits from its top surface through a transparent indium-tin-oxide anode. This device employs a novel protective cap layer which prevents damage to the organic layers during sputter deposition of the anode, while also improving hole injection. Mechanisms of current transport and carrier injection from the contacts are investigated. This device configuration allows for integration of organic light emitting devices with *n*-channel field effect transistors used in display active matrix backplanes. © 1997 American Institute of Physics. [S0003-6951(97)00422-1]

The recent demonstration of efficient electroluminescence (EL) from vacuum-deposited molecular organic light emitting devices (OLEDs)¹ has generated interest in their potential application for emissive flat panel displays. To be useful in low cost, active matrix displays, device structures which are integratable with pixel electronics need to be demonstrated. A conventional OLED is grown on a transparent anode such as indium-tin-oxide (ITO), and the emitted light is viewed through the substrate, complicating integration with electronic components such as silicon-based display drivers. It is therefore desirable to develop an OLED with emission through a top, transparent contact.

Previously, a surface-emitting polymer-based OLED grown on silicon with a transparent ITO and a semitransparent Au or Al top anode was demonstrated.^{2,3} A similar integration of molecular OLEDs with silicon was achieved using a tunneling SiO₂ interface.³ The tunneling interface, however, increases the device operating voltage, and can be avoided in structures such as the recently reported transparent OLED (TOLED)^{4,5} which can, in principle, be grown on a silicon substrate. The TOLED anode, however, forms the bottom contact, whereas for display drivers employing *n*-channel field effect transistors, it is desirable that the bottom contact of the OLED be the cathode. This requires that the ITO anode be sputter-deposited on the relatively fragile hole-conducting organic thin film which can result in unacceptable degradation of the device operating characteristics.

In this work we demonstrate a novel surface-emitting, organic inverted LED (OILED) with a cathode as the bottom contact. This device differs from previously demonstrated surface-emitting OLEDs^{2,3} in that it consists entirely of vacuum-deposited molecular organic materials, and contains a crystalline organic layer that protects the underlying hole-conducting material from damage incurred during sputter deposition of the ITO anode. The protective cap layer (PCL) was not necessary in inverted polymer OLEDs² since the glass transition temperature (T_g) of polymer materials is much higher than T_g of molecular organics, increasing the polymer resistance to damage induced by ITO sputtering. The OILED can be grown on any smooth surface to which the cathode adheres, such as the drain contact of an *n*-channel poly-Si transistor used in active matrix displays.

The OILEDs were fabricated as follows: Prior to deposition of the organic films, (100) Si substrates were cleaned by sequential ultrasonic rinses in detergent solution and deionized water, then boiled in 1,1,1-trichloroethane, rinsed in acetone, and finally boiled in 2-propanol. Between each cleaning step, the substrates were dried in high purity nitrogen. The OILED structure (inset, Fig. 1) was grown starting with the thermal evaporation in vacuum (10^{-6} Torr) of a 1000-Å-thick cathode consisting of 25:1 Mg:Ag alloy, followed by a 500-Å-thick aluminum *tris*(8-hydroxyquinoline) (Alq₃) electron transporting and EL layer, and a 250-Å-thick hole-transporting layer (HTL) of *N,N'*-diphenyl-*N,N'*-bis(3-methylphenyl)-1,1'-biphenyl-4,4'-diamine (TPD). Alternatively, OILEDs employing 4,4'-bis[*N*-(1-naphthyl)-*N*-phenyl-amino] biphenyl (α -NPD) as the HTL were also fabricated, with results similar to those obtained using TPD. To protect the fragile HTL from the sputter deposition of the top, ITO anode contact, either a 3,4,9,10-perylenetetracarboxylic dianhydride (PTCDA) or a copper phthalocyanine

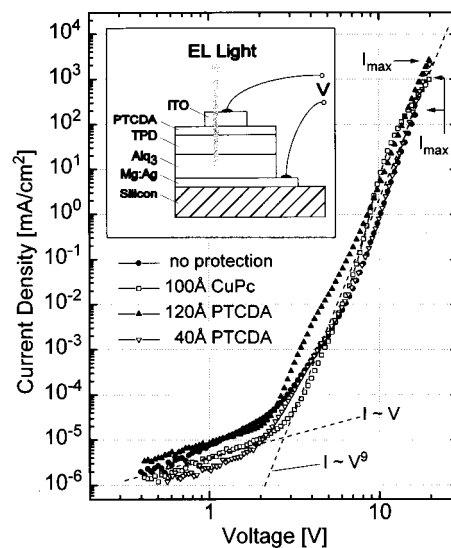


FIG. 1. Forward-biased current-voltage characteristics of 0.05 mm² OILEDs with different protection layer compositions and thicknesses. All devices driven to their maximum current (I_{max}) prior to failure. Inset: Schematic illustration of the OILED structure.

(CuPc) film was employed. Both CuPc⁶ and PTCDA^{7,8} can serve as efficient hole injection layers in conventional OLEDs. Furthermore, the use of PTCDA in a photodetector structure with an ITO electrode deposited on the film surface⁹ has previously demonstrated that this material can withstand sputter-deposition of ITO with minimal degradation to its conducting properties. Typical organic deposition rates ranged from 1 to 5 Å/s with the substrate held at room temperature. Finally, the top, ITO layer was deposited by rf magnetron sputtering of a pressed ITO target in a 2000:1 Ar:O₂ atmosphere, and 5 mTorr pressure. The rf power was 5 W, which resulted in a deposition rate of 200 Å/h.⁵

The forward bias current–voltage (I – V) characteristics of 0.05 mm² OILEDs with PTCDA and CuPc PCLs, as well as of a device with no PCL are compared in Fig. 1. These characteristics are similar to previously reported conventional OLEDs, where trap limited conduction^{7,10,11} ($I \propto V^{(m+1)}$) was observed. For the OILEDs, $m = 8$ independent of the details of the particular device structure or PCL thickness. The EL brightness at a current density of 10 mA/cm² is between 40 and 100 cd/m² for all devices, independent of details of the HTL and PCL anode structure. The OILEDs, whose characteristics are presented in Fig. 1, are a representative sample of devices with different thicknesses of PTCDA or CuPc. The operating voltage of OILEDs employing CuPc as the PCL was independent of CuPc thickness between 40 and 170 Å. In contrast, the operating voltage of PTCDA-protected OILEDs abruptly decreased by 1.5 V as the PTCDA thickness increased from 40 to 60 Å. The voltage drop across the PCL is small compared to that across the rest of the device, since PTCDA and CuPc are both thinner and more conductive⁸ than Alq₃. Therefore, the abrupt change in the I – V characteristics reflects a change in the carrier injection efficiency from the ITO contact. The ITO sputter deposition inflicts film damage to the top-most organic layer. This damage results in only a 30% yield out of 15 devices with no PCL, as compared to 100% yield for devices with either a PTCDA or CuPc PCL. The abrupt increase in the operating voltage for OILEDs with <40-Å-thick PTCDA layers occurs when the thickness of the damaged region is comparable to the PCL thickness. At this point, further deposition of ITO degrades the TPD which becomes directly exposed to the sputtering plasma.

The presence of the PCL also influences the maximum drive current before device breakdown I_{\max} , where I_{\max} for an OILED with no PCL is only 10% of that obtained for OILEDs with either a PTCDA or CuPc PCL. The differences in I_{\max} are evident in both Figs. 1 and 2, where all OILEDs were driven until device breakdown occurred. The PCL therefore both protects the underlying organics, decreases the OILED operating voltage, and increases I_{\max} . A similar decrease in the operating voltage was previously observed for conventional OLEDs with a CuPc-coated ITO anode,⁶ presumably due to a reduced energy barrier to hole injection from the ITO into CuPc as opposed to the energy barrier between the ITO and the HTL. Note that the lowest transition voltage (i.e., the voltage at which ohmic conduction and trap limited conduction are equal) is achieved for OILEDs with >100-Å-thick PTCDA PCLs.

Figure 2 shows the light intensity versus current (L – I)

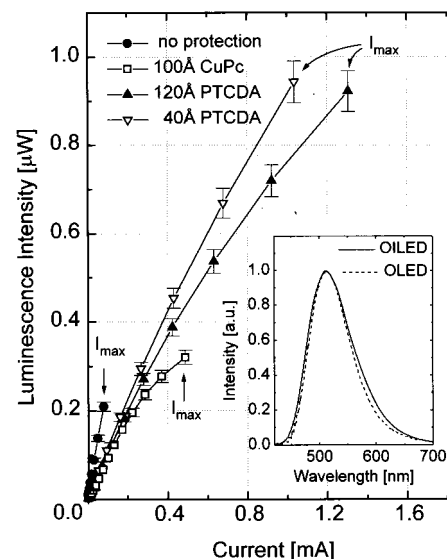


FIG. 2. Light output power–current characteristics of OILEDs with different protection layer composition and thickness. All devices driven to their maximum current (I_{\max}) prior to failure. Inset: The EL spectrum of an OILED with a 60-Å PTCDA PCL and a conventional OLED.

response of the OILEDs in Fig. 1. The external EL quantum efficiency of the protected OILEDs is $\eta = (0.15 \pm 0.01)\%$ vs $\eta = (0.30 \pm 0.02)\%$ for the unprotected devices. This difference is due in part to absorption by the PCL, since both CuPc and PTCDA exhibit a strong absorption at the peak Alq₃ emission wavelength of 530 nm. For example, η decreases by 25% as the CuPc PCL thickness increases from 40 to 170 Å. Similarly, η for PTCDA-protected OILEDs decreases by 25% with an increase in PTCDA film thickness from 10 to 120 Å, consistent with PTCDA absorption. The origin of the remaining difference in η between OILEDs with and without a PCL is not understood, although, we speculate that defects at the PTCDA/ITO interface may scatter a fraction of the emitted light back into the PTCDA where it can experience further absorption. A different PCL material which is transparent to Alq₃ emission is thus expected to increase the OILED efficiency somewhat. The shape of the EL emission spectra of OILEDs with PCLs is similar to that of conventional Alq₃-based OLEDs (inset, Fig. 2). The OILED spectrum with a 60-Å-thick PTCDA PCL is slightly broadened due to the PCL absorption.

To determine the injection efficiency of the ‘‘inverted’’ Mg:Ag/Alq₃ contact, we fabricated Mg:Ag–Alq₃–Mg:Ag devices. Figure 3 shows the I – V characteristics of three such ‘‘symmetric’’ diodes with a 450-Å-thick Alq₃ layer and 0.90, 0.25, and 0.07 mm² top electrodes. An asymmetric response with a larger current in ‘‘forward bias’’ (bottom electrode positive) is clearly apparent, suggesting a different injection efficiency for the top and bottom Mg:Ag/Alq₃ interfaces. This asymmetry is attributed to differences between contact interface chemistries as well as to their roughnesses. Due to their large latent heat of condensation, vapor-deposited Mg and Ag atoms chemically react with the underlying Alq₃ as they thermalize on the film surface, forming interfacial defects which lower the contact energy barrier. In contrast, such reactions are significantly reduced when the relatively

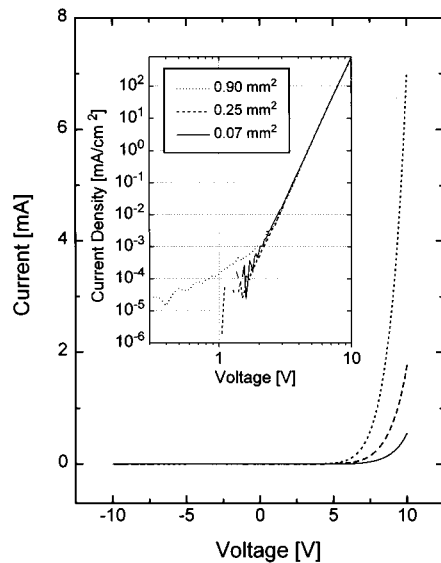


FIG. 3. Current–voltage characteristics of three Mg:Ag–450 Å Alq₃–Mg:Ag structures with 0.90, 0.25, and 0.07 mm² top electrode areas. Voltage is applied to the bottom electrode while the top electrode is grounded. Inset: Forward-biased current–voltage characteristics of the diodes in Fig. 3, normalized with respect to device area.

low sublimation temperature Alq₃ molecules are deposited onto the Mg:Ag surface forming the bottom contact. Since previous studies show that Alq₃ is preferentially electron conducting,^{12,13} the asymmetry implies that the top electrode is a more efficient electron injector into Alq₃ than is the bottom electrode. Since the OILED cathode corresponds to the bottom contact of the Mg:Ag–Alq₃–Mg:Ag sandwich, the carrier injection efficiency is lower in OILEDs as compared to conventional OLEDs, leading to a concomitant increase in the OILED operating voltage. The lower injection efficiency in OILEDs can also be responsible for decreased η , as previously observed in a series of Alq₃ devices using cathodes of various composition.¹⁴

In the inset of Fig. 3, we normalize the forward bias current of the three Mg:Ag–Alq₃–Mg:Ag devices with respect to the top electrode area. The agreement between the normalized I – V characteristics indicates that the current scales with electrode area, suggesting that enhanced electric fields at the contact periphery do not significantly affect the current. We find that $I \propto V^9$, over seven decades of current, consistent with trap-limited conduction in the Alq₃ film.^{7,10,11} The similar I – V power law dependence in Alq₃/TPD-based OLEDs and OILEDs indicates that Alq₃ forms the current limiting layer in all of these devices, when forward biased. The voltage drop over the contact/film interface

region, however, is found to introduce a voltage offset that for a fixed current increases the operating voltage by a constant factor, consistent with previous observations.¹⁴ This indicates that the current in the hole injection/contact region must also follow a power law dependence approximately equal to $I \propto V^9$, characteristic of Alq₃. Comparison of the I – V characteristics in Fig. 3 with those of an OILED with a 120-Å-thick PTCDA PCL (Fig. 1) shows that for currents $> 10^{-3}$ mA/cm², about 60% of the voltage is dropped over the Alq₃ layer, with the remaining voltage distributed over the HTL, PCL, and the contact/film interface regions.

In conclusion, a surface-emitting, or organic “inverted” LED with a cathode as a bottom contact was demonstrated using a novel anode consisting of an organic hole-injecting protection layer and a transparent, sputter-deposited ITO thin film. An OILED can be grown on top of any smooth substrate to which the cathode will adhere, including opaque substrates such as Si and metal foils. The OILED I – V characteristics and EL spectra are similar to those of conventional OLEDs, while the operating voltage is higher and efficiency somewhat decreased, indicating the need for further optimization of the device contacts.

The authors thank Dr. D. Z. Garbuzov for insights into high efficiency OLEDs, Ms. L. Rodriguez for assistance in the growth of single layer Alq₃ devices, C. C. Wu for helpful discussions, and K. Pangal for assistance in SiO₂ growth. The authors also thank DARPA and Universal Display Corporation for their generous support of this research.

- ¹C. W. Tang and S. A. VanSlyke, *Appl. Phys. Lett.* **51**, 913 (1987).
- ²D. R. Baigent, R. N. Marks, N. C. Greenham, R. H. Friend, S. C. Moratti, and A. B. Holmes, *Appl. Phys. Lett.* **65**, 2636 (1994).
- ³H. H. Kim, T. M. Miller, E. H. Westerwick, Y. O. Kim, E. W. Kwock, M. D. Morris, and M. Cerullo, *J. Lightwave Technol.* **12**, 2107 (1994).
- ⁴V. Bulović, G. Gu, P. E. Burrows, M. E. Thompson, and S. R. Forrest, *Nature (London)* **380**, 29 (1996).
- ⁵G. Gu, V. Bulović, P. E. Burrows, S. R. Forrest, and M. E. Thompson, *Appl. Phys. Lett.* **68**, 2606 (1996).
- ⁶S. A. VanSlyke, C. H. Chen, and C. W. Tang, *Appl. Phys. Lett.* **69**, 2160 (1996).
- ⁷P. E. Burrows and S. R. Forrest, *Appl. Phys. Lett.* **64**, 2285 (1994).
- ⁸V. Bulović, P. E. Burrows, S. R. Forrest, J. A. Cronin, and M. E. Thompson, *Chem. Phys.* **210**, 1 (1996); V. Bulović and S. R. Forrest, *Chem. Phys.* **210**, 13 (1996).
- ⁹F. F. So and S. R. Forrest, *IEEE Trans. Electron Devices* **36**, 66 (1989).
- ¹⁰Z. Shen, P. E. Burrows, V. Bulović, D. Z. Garbuzov, D. M. McCarty, M. E. Thompson, and S. R. Forrest, *Jpn. J. Appl. Phys.* **35**, L401 (1996).
- ¹¹P. E. Burrows, Z. Shen, V. Bulović, D. M. McCarty, S. R. Forrest, J. A. Cronin, and M. E. Thompson, *J. Appl. Phys.* **79**, 7991 (1996).
- ¹²C. Hosokawa, H. Tokailin, H. Higashi, and T. Kusumoto, *Appl. Phys. Lett.* **60**, 1220 (1992).
- ¹³R. G. Kepler, P. M. Beeson, S. J. Jacobs, R. A. Anderson, M. B. Sinclair, V. S. Valencia, and P. A. Cahill, *Appl. Phys. Lett.* **66**, 3618 (1995).
- ¹⁴L. S. Hung, C. W. Tang, and M. G. Mason, *Appl. Phys. Lett.* **70**, 152 (1997).